Air Distribution in Rooms, (ROOMVENT 2000)
Editor: H.B. Awbi

13322

FLOW PATTERN IN VENTILATED ROOMS WITH LARGE DEPTH AND WIDTH

Zou Yue[1], Peter V. Nielsen[2]

[1]Department of Building Science Engineering, Royal Institute of Technology (KTH), Sweden
[2]Department of Building Technology and Structural Engineering, Aalborg University, Denmark

ABSTRACT

In many buildings, for instance tunnels, underground, parking areas and industrial halls, the *L/H* is so large that the flow pattern induced by a two dimensional supply air jet along the ceiling can be completely different from that in rooms of normal sizes. Earlier model experiments indicate that, in this case, the supply jet will have a limited penetration length (l_{re}) because the entrainment generates a backward flow in the lower part of the ventilated space which at a given distance will disperse or deflect the jet.

In this study both model experiments and Computational Fluid Dynamics (CFD) are employed to study the isothermal flow pattern in a ventilated room with different *L/H* and inlet velocities. The maximum size of the model is 1.4* 0.72*0.0714*m* and the measurement is made with a Laser Doppler anemometer. The CFD simulation is carried out by Flovent code with a k-ε model. Although some discrepancies occur it is clear that the simulation correctly represents the general features of the measurements. Both measurements and CFD simulations show the tendency that l_{re}/H may be independent of *W/H* when W/H >5. The velocity decay of the wall jet and the maximum velocity in occupied area are also studied in this paper.

KEYWORD

Deep ventilated room, penetration length, CFD, model, wall jet, maximum velocity

INTRODUCTION

In mixing ventilation, wall jets are extensively used for supply of ventilation or conditioned air to rooms and spaces. Before the air enters the occupied area of the room velocities and temperature differences must have decreased to an acceptable level. Considering that the test of supply devices is always done in rooms different from the room where the supply device finally is installed it is of practical interest to study the characteristics of flow in rooms of different sizes.

For rooms with small characteristic dimensions (*W/H < 2, L/H < 3*), where *W, L* and *H* are width, length and height of the ventilated space, the wall jet undergoes a number of deflections at the corners it meets during its course from the supply to the floor. When the jet is approaching an opposing side (room corner), an adverse pressure gradient is built up and the jet "restarts" again, see Sandberg (1998). When the ratio *L/H* is larger than a certain value, entrainment implies that the air must be led back along the floor and this will disperse the jet. The distance from the wall with the inlet to the stagnation point where the flow diverges is called penetration length l_{re}, see figure 1. The penetration length is a significant parameter for proper room air distribution design. At a distance from the supply opening which is larger than l_{re} the velocity is very low since the supply air is distributed over the whole cross area, while the velocities are very high at distances smaller than l_{re} because large volume of air is set into motion by the entrainment below the wall jet. For a normal room the ventilated section should always be smaller than the calculated penetration length so a rotary airflow pattern can be established. However, some applications, such as mining tunnels, require a penetration length as long as possible. Therefore, there is a need for a procedure which allows the penetration length and the velocity distribution to be determined as a function of the room geometry and the inlet condition. The results presented here demonstrate that this can be achieved by the CFD simulation.

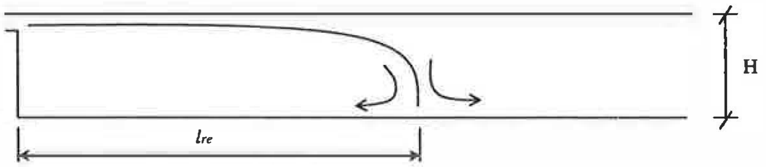

Figure 1: Penetration length of long room.

Experimental investigations of the penetration length can be found in e. g. Urbach (1971), Katz (1974), Förthmann (1934), Nielsen (1976) and Nielsen et al. (1987). With the aid of smoke visualization Urbach (1971) makes tests in a model with W/H =1 and found value of l_{re}/H about 3 for h/H between 0.02 and 0.1 and Reynolds number between 3500 and 12000. Katz's (1974) experiments were also carried out with small W/H but in an open water channel. His tests showed that the penetration length is somewhat dependent on the location of the end wall and l_{re}/H was found between 3 and 4.5. In Förthmann (1934) the velocity profiles in a deep model with h/H = 0.17 and W/H = 3.6 were measured. Based on these data l_{re}/H was calculated as 5.3. Nielsen et al. (1987) investigated air distribution in rooms with ceiling-mounted obstacles and found that penetration length can be strongly influenced in some cases. Detailed tests of penetration length with different model geometric parameter can be found in Nielsen (1976). Some of them will later be discussed.

EXPERIMENT SETUP AND SIMULATION

The measurements were performed in a model as shown in figure 2 which also indicates the coordinate system used. This model was made from perspex and a full-width slot was placed just below the ceiling. Supply air was led into the model by a ventilator located downstream of the exhaust air terminal device to make sure the tests were held under isothermal conditions. The supply outlet was also preceded by a smooth curved area contraction to produce a uniform velocity profile and reduce the turbulence level. To determine the influence of width and length on the velocity characteristics two different model sizes were applied in the tests. Geometric parameters of these two models are summarized in table 1. For all tests the supply air velocity is 15.1 *m/s*, corresponding to a Reynolds number about 4000. The measurements of mean velocities and the corresponding turbulence intensities were carried out by a Laser Doppler anemometer. The minimum measurement time for each point is 30 seconds.

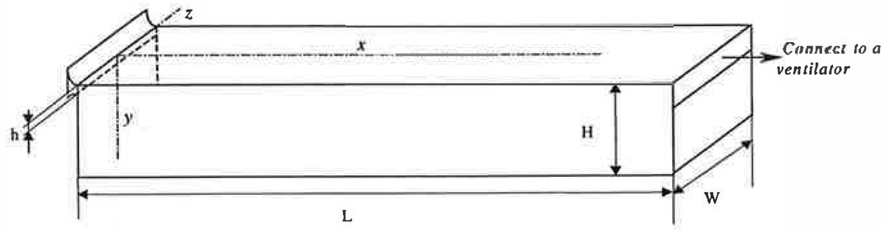

Figure 2: Layout of model

TABLE 1
MODEL DIMENSIONS

	H	h	h/H	L/H	W/H
Model 1	7.14 cm	4mm	0.056	20	10
Model 2	7.14cm	4mm	0.056	15	5

The CFD simulations were carried out under steady state conditions. The flow field was divided into a collection of small rectangular cells and the flow at each cell is determined by numerically solving the governing conservation equations of fluid dynamics. The grid density was 80*50*80 grids along the length (x), height (y), width (z), respectively. The grids have smaller spacing at locations where more flow detail are needed (the supply and the jet flow area). Turbulence is modelled by a standard k-• model. For all cases, in the absence of turbulence data, the turbulence intensity at inlet is assumed to be 4% and the turbulence kinetic energy k and its dissipation rate ε at the inlet are determined by

$$k = \frac{3}{2}(IU_o)^2 \tag{1}$$

$$\varepsilon = \frac{0.09k^{3/2}}{h} \tag{2}$$

where

I = Relative turbulence intensity (-)
U_O = Outlet velocity evaluated from the estimated mass flow (m/s)

RESULTS AND DISCUSSION

Flow pattern and comparison

Figure 3 presents profiles of the longitudinal velocity component at three x and z positions measured in model 2. As it can be seen, the flow pattern is two-dimensional at $x/H=2.8$. However, the flow is not always symmetric around the mid plane (within measurement precision) at other positions. This fact indicates that care must be taken when making tests which only represent a part of a room.

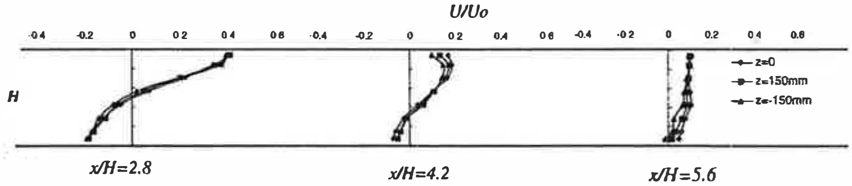

Figure 3: Measured mean velocity profile at different x and z positions

In a model with similar characteristic size (W/H=4.7) to model two, Nielsen (1976) observed that an instantaneous flow occurred in the z direction for flow between x/H =4.2 *and* 5. In our test, such evidence is not found. However, the RMS (*Root Mean Square*) value of the longitudinal velocity component at y=4mm of model 2 had a peak value in this area, see figure 4.

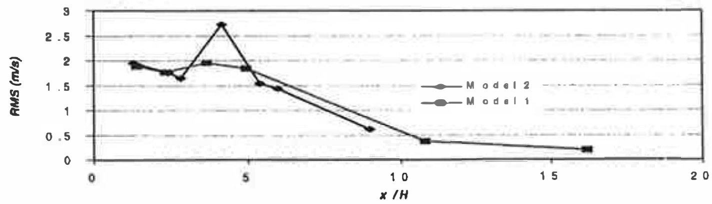

Figure 4: RMS value distribution along then centreline at 4mm from the top for model 1 and 2

Three-dimensional CFD simulations show that the flow patterns in both models are close to be two-dimensional. No evidence of non-symmetry around the mid plane can be found. In figure 5 comparisons of both velocity profile and velocity distribution at ceiling level and floor level along the centre line in the model 1 are presented. Although some discrepancies occur it is clear that the simulation correctly represents the general features of the measurements.

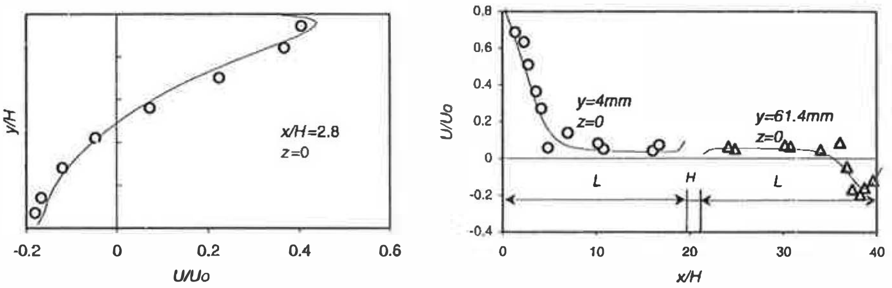

Figure 5: Comparisons in velocity profile (a) and velocity distribution (b) along the centreline in the model 1

Penetration length

Dimensional analysis indicates that the flow in a ventilated room can be described by the geometrical parameters, the Reynolds number Re and the boundary conditions, see Nielsen (1976). Therefore the penetration length can be expressed as:

$$\frac{l_{re}}{H} = f\left(\frac{W}{H}, \frac{L}{H}, \frac{h}{H}, \mathrm{Re}\right) \tag{3}$$

where three variables on the right hand side represent the geometry normalized by the height of the room. The Reynolds number is given by

$$\mathrm{Re} = \frac{U_o h}{\nu} \tag{4}$$

where ν is the kinematic viscosity

For a fully developed turbulent flow the normalized velocity distribution in ventilated rooms is independent of the Reynolds number, see Nielsen (1976) and Sandberg et al (1998). Figure 6 shows that the normalized return flow in the model expressed by the ratio U/U_o in model 1 at y = 6.64cm and x = 20cm is almost independent of the Reynolds number for $\mathrm{Re} \geq 4000$.

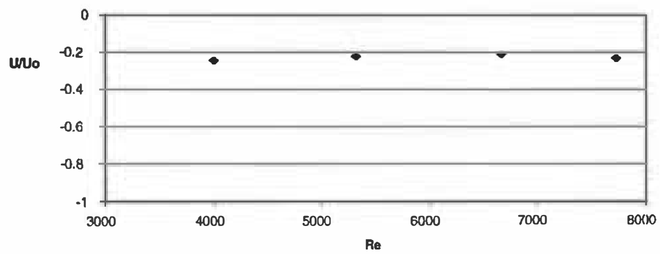

Figure 6: Normalized velocities in model 1 at 5mm from bottom and 20cm from supply outlet for different outlet Reynolds numbers

According to measurement data at 0.5 cm from bottom the penetration lengths in both model 1 and model 2 are estimated to be between 4.5 H and 5 H while CFD calculations give 5.9 H and 5.6 H for model 1 and 2, respectively. In figure 7 available penetration length data is presented for different *W/H* and a best-fitted line for penetration length for all measurements with $h/H = 0.056$ is also given. This line shows a tendency that l_{re}/H may be independent of *W/H* when W/H >5.

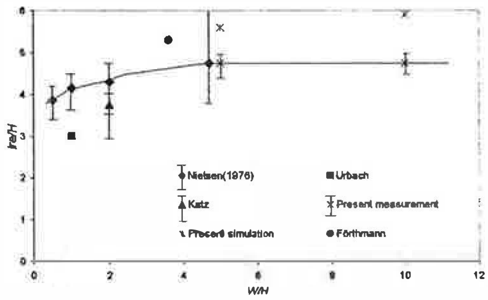

Figure 7: Penetration length versus *W/H*

Velocity Distribution

In figure 8 the normalized maximum measurement velocities U_m / U_o of model 2 are plotted log-log as a function of the normalized distance from the inlet *x/h*. The velocity decay has a slope of –0,5 in the first part. Obviously this part belongs to the zone of fully established turbulent flow where the maximum velocities can be expressed as:

$$\frac{U_m}{U_o} = K\sqrt{\frac{h}{x + x_o}} \tag{5}$$

where

K = Velocity decay coefficient for wall jet
x_o = Distance to virtual origin

In this test, K and x_o are found to be 3 and 25mm which is in agreement with other experiments, see Malmstrom (1974).

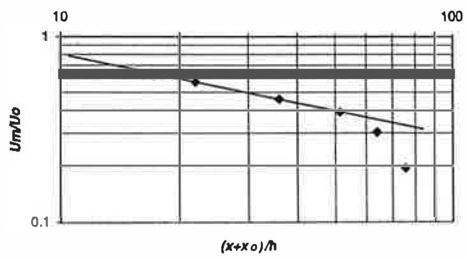

Figure 8: Maximum velocity decay for wall jet

The maximum velocity in the occupied zone U_{rm} is another important parameter in the design of an air distribution system. In a "shorter" room with mixing ventilation this maximum velocity is located close to the floor at *2/3L* from the inlet, see Zou (1999). Table 2 shows that data of U_{rm} and the locations of

U_{rm} from the inlet x_{rm} are related to the penetration length. It is interesting to note that the measured data of x_{rm}/l_{re} are also close to *2/3*.

TABLE 2
MAXIMUM VELOCITY IN OCCUPIED AREA

		U_{rm}/U_0	x_{rm}	l_{re}	x_{rm}/l_{re}
Model 1	Measurement	-0.2	2.8*H*	4.5*H*-5*H*	0.56-0.63
	simulation	-0.17	2.4*H*	5.9*H*	0.41
Model 2	Measurement	-0.19	2.8*H*	4.5*H*-5*H*	0.56-0.63
	simulation	-0.17	2.4*H*	5.6*H*	0.43

Conclusion

In this study both model experiments and Computational Fluid Dynamics (CFD) are carried out to study the isothermal flow pattern in the ventilated room with different *L/H* and supply air velocities. Although some discrepancies occur it is clear that the simulation correctly represents the general features of the measurements. Both measurement and CFD simulation show a tendency that l_{re}/H may be independent of *W/H* when W/H >5. The maximum velocity decay of the wall jet and the maximum velocity in the occupied area are also studied in this paper.

Acknowledgement

The measurement part of this work is made in cooperation with one student group in Aalborg University, Denmark. The first author would also like to thank Aalborg University that sponsored this project.

REFERENCES

Förthmann E. (1934). Über turbulente Strahlausbreitung. Ing. Archiv 5.

Katz P. (1974). Wurfweite, Eindringtiefe und Lauflänge von Zuluftstrahlen im klimatisierten Raum. *HLH* **No. 3**.

Malmström T.-G. (1974). Om Funktionen hos Tilluftsgaller. *TM* **49**, Department for Heating and Ventilation, KTH, Stockholm, Sweden.

Nielsen P.V.(1976). *Flow in Air Conditioned Rooms*, PhD thesis, DTH, Copenhagen

Nielsen P.V., EvensenL., Grabau P. and Thulesen-Dahl J. H. (1987). Air Distribution in Rooms with Ceiling-Mounted Obstacles and Three-Dimensional Isothermal Flow. *ROOVENT 87*, Stockholm

Nielsen P.V. (1995). *Lecture Note on Mixing Ventilation*. Dept. of building technology and structural engineering, Aalborg University, Demark

Sandberg M. (1998). Some Confinement Effects of Jets in Ventilated Rooms. *ASHRAE Transaction*, **SF-98-28-2**, pp 1748-1754

Sforza P.M. (1977). Three-Dimensional Free Jet and Wall Jet: Application to Heating and Ventilation. *ICHMT Congress*, "Heat transfer in buildings", Dubrovnik

Urbach, D.(1971). *Modelluntersuchungen zur Strahllüftung*, Diss. RWTH Aachen

Zou, Y. (1999). A CFD Study for Airflow Distribution at Floor Level in a Slot-Outlet and Slot-Inlet Ventilation Room. *The 3rd International Symposium on HVAC*, Shenzhen, China